

Detection of Land Surface Temperature in Relation to Land Use Land Cover Change: Dire Dawa City, Ethiopia

Matiwos Belayhun Haylemariyam*

Dire Dawa University, Dire Dawa, Ethiopia

*Corresponding author: Matiwos Belayhun Haylemariyam, Dire Dawa University, Dire Dawa, Ethiopia, Tel: +251904137334; E-mail: matibelahun1212@gmail.com

Rec date: June 25, 2018; Acc date: July 19, 2018; Pub date: July 24, 2018

Copyright: © 2018 Haylemariyam MB. This is an open-access article distributed under the terms of the Creative Commons Attribution License, which permits unrestricted use, distribution, and reproduction in any medium, provided the original author and source are credited.

Abstract

The study used Landsat 5 TM acquired on August 1993 and Landsat 8 OLI/TIRS acquired on September 2017 to retrieve satellite brightness temperature and analyzing land use land cover change and its impact on land surface temperature of Dire Dawa City, Ethiopia. The land use/land cover classification was made using maximum likelihood algorithm and five major land use land cover (Built up, barren land, shrub land, sparse vegetation and Dry River) were identified. The land use land cover result reveal built up and shrub land area have been expanding rapidly and barren land has shown decreasing trend in areal extent. On the other side, result of the study shows, barren land and built up area exhibit highest mean value of land surface temperature. Shrub and sparse vegetation land use land cover class exhibit lowest mean land surface temperature, as they are vegetative cover. Areas with high vegetation cover or Normalized Difference Vegetation Index value often depict high land surface temperature and therefore, NDVI have strong negative correlation with land surface temperature. From the study, it is identified that, the change in land use land cover because of urban growth, settlement expansion and construction of new built up or dwelling units in the city, leads to increment in land surface temperature. As a result, urban growth has resulted in the change of land surface temperature.

Keywords: Land use; Land cover change; Land surface temperature; NDVI

Introduction

Our planet earth and its environment have been modified for thousands of years due to human induced activities. These environmental changes are intensified by high population pressure, migration, and socio-economic activities. The changes have been found in various spatial scale from local to global level [1]. Large-scale human activities like agriculture and settlement expansion are continuously decreasing the vegetative cover of the earth's surface. Consequently, the concentration of carbon dioxide is increasing in the atmosphere which in turn affecting the surface energy budget thereby producing changes in local, regional and global climate [2].

Uncontrolled population growth and the rapid development of world-wide urbanization have an extreme impact on the environment [3]. Urbanization has been increased from time to time with the escalation of population number and rural-urban migration particularly in developing countries. The process of urbanization is concerned with the conversion of land use/land cover. These conversion in arable land to paved surface has resulted in decline in natural land cover especially vegetation. Rapid urbanization process brought about many eco-environmental problems, such as the drastic change of land use and development of urban heat island [4]. Urban development coupled with unsustainable land management practices has a great impact on the local climate of a city. The abrupt land cover changes modify amount of absorption of solar radiation, evaporation rates, thermal storage of surfaces and wind turbulence (Estimation of Spatial Variability of Land Surface Temperature using Landsat 8 Imagery, 2015). Exploitation of the natural environment by human being through urban development and expansion has a major impact

on the urban microclimate at local and global climate in wider scale. One major phenomenon that arises as a result of this exploitation is the increase in land surface temperature [5].

The change of land use is the important reasons leading to increase in land surface temperature. Land use/cover is very important factor having a significant impact on Earth ecosystem [6]. Land use/land cover changes significantly alter the surface energy budgets of urban area. It also brought a change in urban morphology and urban micro climate [7]. Surface temperature has increased due to transformation of land use/land cover classes into non-evaporating surfaces. Land surface temperature has increased due to transformation of deposition and open forest into settlement [8].

Urban land development has an impact on urban climate particularly it raised surface temperature [9,10]. The direct effect of urban land use/cover change on one environmental element can cause indirect effect on the other. The increase of surface radiant temperature is related to the decrease of biomass.

GIS and remote sensing techniques have shown their importance in mapping urban land use/land cover, urban growth trends to monitor the changes in land use/land cover [11]. The integration of remote sensing and GIS was found to be effective in monitoring and analyzing urban growth patterns and in evaluating urbanization impact on surface temperature. The digital image classification coupled with GIS has demonstrated its ability to provide comprehensive information on the nature, rate and location of urban land expansion and its associated land surface temperature increment. Biophysical measurements including surface radiant temperature and biomass can be extracted from imagery [9]. Using remote sensing technique, the alteration of change in urban land cover on spectral signature and emissivity of land surface can be detected [5]. The land use change (urbanization) led to the migration of pixels from cool to hot surface

condition [4,8]. Remote sensing images therefore, can be serving as a source of data to the monitoring of LULC changes and its dynamics over different time scales that occur on urban areas. It has also an indispensable value to the estimation of LST using thermal band.

Multi temporal digital satellite imagery enable to extract information about land use land cover and land surface temperature which intern are crucial for urban land management decision-making, ecosystem monitoring and urban planning [3]. Thus, remote sensing data has been found to be effective in analyzing urban-land surface temperature relationships [12]. Moreover, satellite-based studies can aid urban planners in providing recommendations for building design and landscaping of urban developments that are useful in minimizing the heat accumulation and retention by urban surfaces [2].

Study Area

Dire Dawa City is located in Eastern part of the country on the boarder of Awash plain and on the Eastern highland just at foot slope of the Dengego mountain between 9027' and 9049'N Latitude and 41038' and 42019'E Longitude (Figure 1). The city is surrounded by Oromia National Regional State to the Eastern, Western, Northern, and Southern sides, while the Somali National Regional State bounded in the east. Dire Dawa city is found at 515 km. East of Addis Ababa. It consists of nine urban administrative sub-units (kebeles). The city is totally located in the Awash River Basin and the altitudinal ranges varies from 950 to 2,260 masl. In the south, it comprises the main escarpment of the eastern edge of Harerghe highlands. Dire Dawa is one of the largest and modern cities of Ethiopia. According to Dire Dawa Administration statistical report, in 2015 the city has a total population of 274,292 [13].

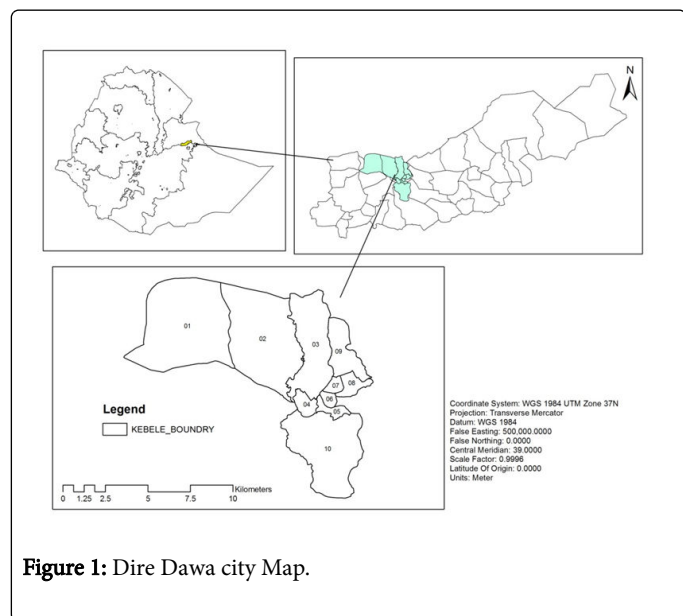


Figure 1: Dire Dawa city Map.

Database and Methods

Image acqizition and pre-processing

Landsat satellite images (Landsat 5 TM, acquired on August 1993 and Landsat 8 OLI/TIRS images, acquired on September 2017) with metadata (MTL) file for the study area (Path/Row 166/53) downloaded from Earth Explorer website and used for assessing land use land cover

(LULC) change and their impact for land surface temperature (LST). Image pre processing which comprises layer stacking, image enhancement, band combination, and false color combination were applied to the images. The images were rectified to WGS-1984-UTM-Zone 37N. Thermal band (Band 6 for TM sensor and Band 10 and 11 for OLI/TIRS sensor) were used to calculate At-Satellite Brightness Temperature. In addition, LST and Normalized Difference Vegetation Index (NDVI) for each year were computed to observe the change of LST induced by land use land cover change.

Image classification

According to Dire Dawa Administrative Council and Office the land use/land cover types have been grouped into four major classes. They are designated as urban built up, physiognomic vegetation types, cultivated land, and bare land [14]. In line with the major class identified by the office, the study adopts five major classes, which comprise Built up, Dry River, Barren Land, Sparse vegetation, and Shrub land (Table 1).

No	Type of LULC	Description
1	Urban and/or Built up Area	An area of human habitation developed due to non agricultural use and that which have buildings classified into different categories like residential, recreational, industrial transport, communication, utilities etc
2	Shrub land	Area which is covered with dense shrub, open shrub land (<i>Prosopis Juliflora</i> plantation) and Eucalyptus plantation
3	Sparse vegetation	Lands with a mosaic of forests, woody plants, trees, natural vegetation, gardens, parks and vegetated lands, agricultural lands, and crop fields
4	Barren land	Open spaces, bare lands and soils, sands, dunes and excavation sites

Table 1: Land use land cover class and its description.

Data Sets Used

Conversion of digital number to radiance

The first step to compute LST was conversion of the digital number in to radiance for TM sensor (Table 2). Therefore, from metadata file, digital number of TM sensor was converted in to radiance value using the following equation.

$$L\lambda = ((LMAX\lambda - LMIN\lambda) / (QCALMAX - QCALMIN)) * (QCAL - QCALMIN) + LMIN\lambda \quad (1)$$

Where:

$L\lambda$ = Spectral Radiance at the sensor's aperture in watts/(meter squared × ster × μm)

$LMIN\lambda$ = the spectral radiance that is scaled to QCALMIN in watts/(meter squared × ster × μm)

$LMAX\lambda$ = the spectral radiance that is scaled to QCALMAX in watts/(meter squared × ster × μm)

$QCALMIN$ = the minimum quantized calibrated pixel value (corresponding to $LMIN\lambda$) in DN

QCALMAX=the maximum quantized calibrated pixel value (corresponding to LMAXλ) in DN

QCAL=the quantized calibrated pixel value in DN

TM Sensor	Thermal Band 6
RADIANCE_MAXIMUM	15.303
RADIANCE_MINIMUM	1.238
QUANTIZE_CAL_MAX	255
QUANTIZE_CAL_MIN	1

Table 2: TM sensor radiance and quantized calibrated pixel.

OLI and TIRS thermal bands (Band 10 and Band 11) data were converted to Top of the Atmosphere (TOA) spectral radiance using the radiance rescaling factors provided in the metadata file (Table 3). Hence, digital number for Landsat 8 imagery of thermal band is computed to generate radiance using equation below.

$$L\lambda = MLQcal + AL \quad (2)$$

Where:

$L\lambda$ =TOA spectral radiance (Watts/ (m² × srad × μm)),

ML=Band-specific multiplicative rescaling factor from the metadata (RADIANCE_MULT_BAND_x, where x is the band number),

AL=Band-specific additive rescaling factor from the metadata (RADIANCE_ADD_BAND_x, where x is the band number),

Qcal=Quantized and calibrated standard product pixel values (DN).

Thermal Band	Radiance_mult_band	Radiance_add_band
Band 10	3.3420	0.10000
Band 11	3.3420	0.10000

Table 3: OLI/TIRS sensor multiplicative and additive rescaling factor.

Conversion of radiance to At-Satellite temperature

Radiance value of TM sensor (Table 4) that is computed from equation 1 was converted in to At satellite temperature in Kelvin using the following equation.

$$T = \frac{k2}{\ln\left(\frac{K1}{L\lambda} + 1\right)} \quad (3)$$

Where:

T=Effective at-satellite temperature in Kelvin,

K2=Calibration constant 2,

K1=Calibration constant 1,

L=Spectral radiance in watts/(meter squared × ster × μm).

TM Thermal Band Calibration Constants		
TM sensor	Constant 1- K1 watts/(meter squared ster × μm)	Constant 2- K2 Kelvin watts/(meter squared × ster × μm)

	607.76	1260.56
--	--------	---------

Table 4: TM sensor thermal band calibration constants.

Similar to TM data, OLI/TIRS thermal band data was also converted from spectral radiance (Table 5) (derived using equation 2) to top of atmosphere brightness temperature using the thermal constants provided in the metadata file:

$$T = \frac{k2}{\ln\left(\frac{K1}{L\lambda} + 1\right)} \quad (4)$$

Where:

T=Top of atmosphere brightness temperature (K),

$L\lambda$ =TOA spectral radiance (Watts/(m² × srad × μm)),

K1=Band-specific thermal conversion constant from the metadata (K1_CONSTANT_BAND_x, where x is the thermal band number),

K2=Band-specific thermal conversion constant from the metadata (K2_CONSTANT_BAND_x, where x is the thermal band number).

Thermal Band	K1_Constant_Band	K2_Constant_Band
Band 10	774.885	1321.08
Band 11	480.888	1201.14

Table 5: OLI/TIRS sensor specific thermal conversion constant.

The average of two bands (Band 10 and Band 11) At satellite temperature were calculated since two thermal bands of Landsat 8 are used for this study.

Conversion of Kelvin to Celsius

°C=T-273.15 where T=at satellite temperature computed from equation 3 and equation 4 for both TM and OLI/TIRS sensors.

Normalized Difference Vegetation Index (NDVI): Normalized difference vegetation index was used to calculate land surface emissivity of both study years. Hence, NDVI for landsat TM, 1993 and Landsat OLI/TIRS, 2017 was computed. Accordingly, the following formula was employed to calculate NDVI.

$$NDVI_{TM} = \frac{Band\ 4 - Band\ 3}{Band\ 4 + Band\ 3}$$

Where band 4 is Near Infrared (NIR) and band 3 is Red.

$$NDVI_{Landsat\ 8} = \frac{Band5 - Band4}{Band5 + Band4}$$

Where Band 5 is Near Infrared and Band 4 is Red

Retrieving of land surface emissivity: Land surface emissivity is retrieved after NDVI has calculated. Land surface emissivity of the two sensor imagery was calculated via the following formula.

$$e = 0.004 PV + 0.986 \quad (5)$$

Where e=Land surface emissivity,

Pv=Proportion of vegetation,

$$PV = \frac{NDVI - NDVI_{min}}{NDVI_{max} - NDVI_{min}} \quad (6),$$

Where NDVI min=minimum value of NDVI,
 NDVI max=maximum value of NDVI.

Land Surface Temperature (LST)

$$Land\ surface\ temperature\ (LST) = \frac{BT}{1} + w \times \frac{BT}{p} \times Ln(e) \quad (7)$$

Where

BT=at satellite temperature,

w=wavelength of emitted radiance.

$$p = \frac{h \times C}{s} (1.438 \times 10^{-2} mK)$$

h=plank's constant (6.626×10^{-34} JS),

s=Boltzmann constant (1.38×10^{-23} J/K),

c=velocity of light (2.998×10^8 m/s and p=14380).

Land surface temperature of 2017 was calculated by taking the average of two thermal bands (band 10 and 11) from landsat 8 OLI/TIRS.

Results and Discussion

Analysis of land use/ land cover (LULC)

Based on the land use/land cover class type adopted from Dire Dawa Agriculture Bureau, five major classes were classified for both study years (1993 and 2017). The classification is intended to produce land use land cover change for 25 years and compare against land surface temperature change.

Class No.	Class Name	LULC, 1993		LULC, 2017	
		Count	Area/km ²	Count	Area/km ²
1	Built Up	14183	3.19	25499	5.74
2	Sparse Vegetation	12328	2.77	3544	0.8
3	Shrub Land	18157	4.09	29976	6.74
4	Barren Land	48705	10.96	34666	7.8
5	Dry River	1159	0.26	520	0.12

Table 6: Land Use/Land Cover (LULC) 1993-2017.

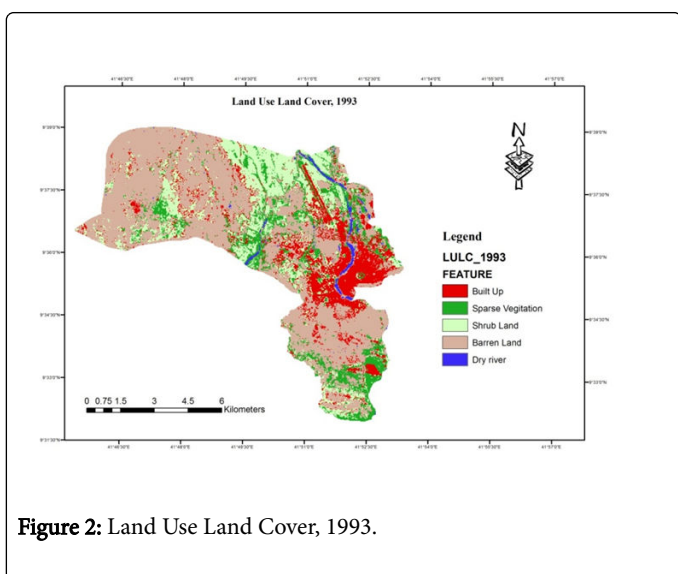


Figure 2: Land Use Land Cover, 1993.

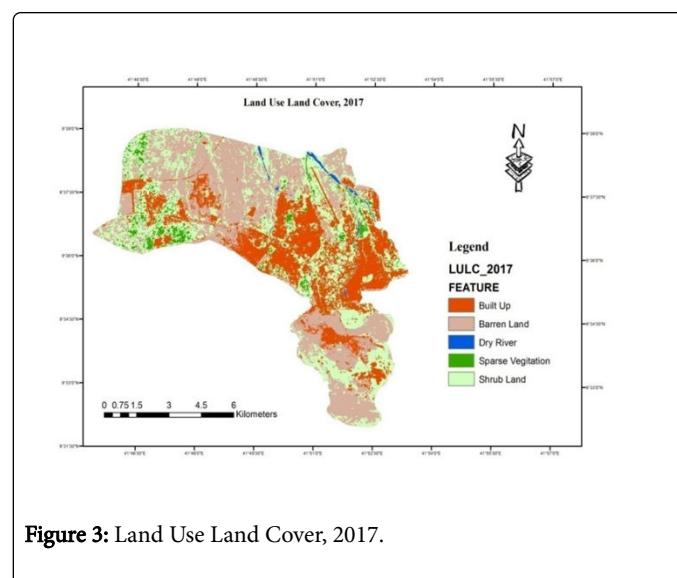


Figure 3: Land Use Land Cover, 2017.

Land use land cover map of Dire Dawa city for 1993 and 2017 study years with five major categories namely built up, barren land, shrub land, sparse vegetation and Dry River were generated. The supervised maximum likelihood was applied and total area with its percentage was calculated. According to Table 6 and Figures 2 and 3, in 1993, LULC of barren land (10.96 sq. Km) and shrub land (4.09 sq. Km) takes the largest share followed by built up area (3.19 sq. Km) and sparse vegetation (2.77 sq. Km).

The least share of LULC category was Dry River with a total area of 0.26 sq. Km. In 2017 or after 25 years, synonymously with 1993, the total area of barren land is greater (7.8 sq. Km) and followed by shrub land (6.74 sq. Km). Built up area had grew more having a total area of 5.74 sq. Km and Dry River (0.12 sq. Km). Therefore, in both study years the dominant class of LULC was Barren land followed by shrub land and built up area. On the other hand, the above table also depicts that, the least dominant type of LULC was Dry River. LULC changes of

25 years were calculated using change detection matrix to point out the rate of change and conversion. Evidently, Table 7 shows, for the last 25 years there has been a drastic increase in areal extent and coverage of shrub land class from 4.09 sq. Km (15%) to 6.74 sq. Km (31.79%)

followed by urban built up area 3.19 sq. Km (15%) to 5.74 sq. Km (27.07%). Shrub land and built up area has shown an increment in 2.65 sq Km and 1.84 sq. Km respectively.

Class No.	Class Name	LULC 1993		LULC 2017		Difference /km ²
		Area/km ²	Percentage	Area/km ²	Percentage	
1	Built Up	3.19	15	5.74	27.07	+1.84
2	Sparse Vegetation	2.77	13	0.8	3.77	-1.97
3	Shrub Land	4.09	19	6.74	31.79	+2.65
4	Barren Land	10.96	51.5	7.8	36.79	-3.16
5	Dry River	0.26	1.5	0.12	0.58	-0.14
	Total	21.27	100	21.2	100	

Table 7: LULC Change 1993-2017.

In contrary to shrub land and built up, barren land has shown a considerable decrease in areal extent from 10.96 sq. Km (51.5%) in 1993 to 7.8 sq. Km (36.79%) in 2017. Thus, a total area of 3.16 sq. Km has been converted in to other LULC class. In addition, sparse vegetation has been steadily decline from 2.77 sq. Km (13%) in 1993 to 0.8 sq. Km (3.77%) in 2017. Consequently, 1.97 sq. Km sparse vegetated area were converted in to shrub land and built up area. Even though it is minimum in comparison with sparse vegetation, Dry River has been shown a slight reduction from 0.26 sq. Km (1.5%) in 1993 to 0.12 sq. Km (0.58%) in 2017 with a total area of 0.14 sq. Km.

With regard to shrub land, for the last three decades it has been expanded rapidly. Particularly, alien plant species named *Prosopis juliflora* scores fast rate of expansion. *Prosopis juliflora* is a permanent dry land tree or shrub, fast growing, often ever green and drought resistant plant of desert and semi desert areas and it is now a serious topic in Ethiopia especially in Dire Dawa [15,16]. The rate of expansion of *Prosopis juliflora* species is alarming and fast in nature [17]. According to Dire Dawa city municipal office the most dominant tree species identified include *Prosopis juliflora*, *Tamarix aphylla*, *Calotropis procera*, *Parkinsonia aculeata*, *Balanites aegyptica*, *Dodonaea*, *Acacia spp.*, *Combratum molle* and *Azadirachta indica* [18]. From those identified tree species, *Prosopis juliflora* is the most common and rapidly invading tree. From invasive plant, *Prosopis juliflora* has a characteristic of vigorous growth, which helps them to compete with indigenous plant species to cover huge areas of land in a relatively short period.

Built up area is the second LULC class that shows rapid expansion next to shrub land. It is parent that, the expansion of settlement is due to high population growth and rural urban migration which accompanied with informal settlement [19,20]. In the first census 1984,

the total population of the city was 99,980 and in the second census 1994, it was grown to 173. In the third census the population number was increased to 188 2007 233, 224. The total population of the city in 2015 was 274, 292 [13]. Therefore, population size have been increasing from time to time Hence, due to the growth of Dire Dawa city, built up area has been considerably grown and barren land has been converted in to built up.

On the other side, the deterioration of barren land for the last 25 years as shown in the above Table 7 and Figures 2 and 3 is due to horizontal expansion of settlement (built up) with construction of new dwelling units, infrastructure (roads and pavements) and industries. In addition, rocky land and sandy areas has been invaded by *Prosopis juliflora*. With respect to sparse vegetation, the main driver of decrease in areal coverage is related to high rate of deforestation and clearance of vegetation for charcoal production and settlement expansion. Particularly, acacia wood land have been degraded for charcoal production in which significant number of rural people use it as a means of livelihood.

The areal extent of Dry River was shrinking from 1993 to 2017. The main driver for deterioration of this land use type is river banks are the main spot area where slum settlements are dominated in Dire Dawa city. In addition, temporary petty market place, which is characterized by sub- standardized shades, is constructed and resides inside the Dry River. Slum settlement often prefer hazardous locations, flood zone and river areas [21]. Consequently, Dry River is converted in to slum area, petty market site, and built up.

Analysis of Normalized Difference Vegetation Index

Class No.	Class Name	NDVI, 1993				NDVI, 2017			
		Min	Max	Mean NDVI	STD	Min	Max	Mean NDVI	STD
1	Built Up	-0.2193	0.66	0.1069	0.0694	0.0452	0.2422	0.1329	0.0213

2	Sparse Vegetation	0.105	0.8102	0.1825	0.094	0.1273	0.2875	0.1921	0.0229
3	Shrub Land	0.0815	0.4407	0.2259	0.0593	0.0915	0.2901	0.155	0.0212
4	Barren Land	-0.1209	0.3676	0.0878	0.0334	0.0779	0.2048	0.1287	0.012
5	Dry River	0	0.0879	0.0332	0.0192	0.107	0.1636	0.1223	0.0075

Table 8: Normalized Difference Vegetation Index 1993-2017.

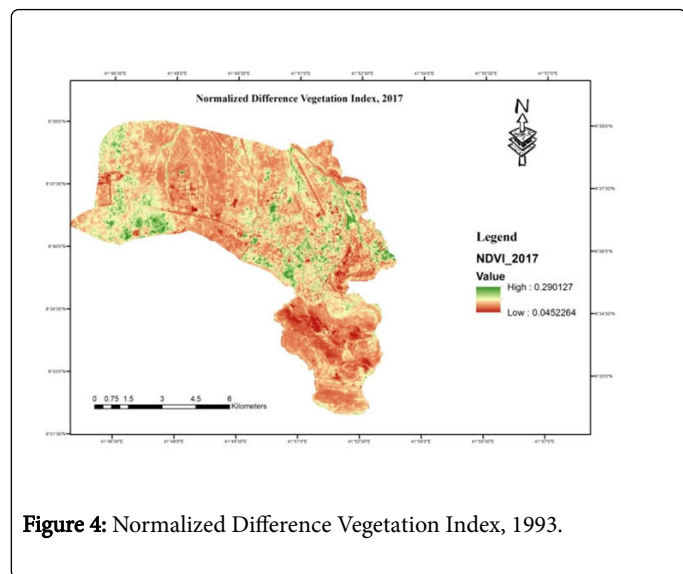


Figure 4: Normalized Difference Vegetation Index, 1993.

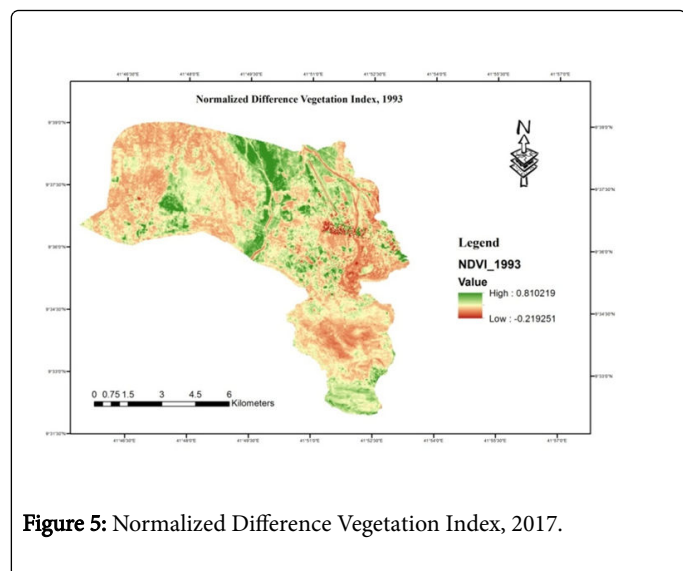


Figure 5: Normalized Difference Vegetation Index, 2017.

The vegetation cover of Dire Dawa city is quantified and extracted from remotely sensed images of 1993 and 2017. The value of NDVI

ranges from +1 to -1 where positive value indicates high vegetation cover and negative value indicates less vegetated area. Very low value of NDVI (0.1 and below) correspond to barren areas of rock, sand, or snow. Moderate values represent shrub and grassland (0.2 to 0.3), while high value corresponds to dense vegetation (0.6 to 0.8). Bare soil is represented with NDVI values, which are closest to 0 and water bodies are represented with negative NDVI values [22]. Table 8, Figures 4 and 5 reveal that, the highest NDVI value for 1993 was 0.81 and lowest negative value of 0.21 was recorded. In 2017, highest NDVI was 0.29 and lowest was 0.045.

In comparison to each LULC class in 1993, Dry River has shown lowest mean value of NDVI 0.0332 followed by barren land 0.0878 and built up 0.1069. During the same study year, shrub land recorded highest NDVI mean value of 0.2259 followed by sparse vegetation 0.1825. In 2017, the NDVI mean value of sparse vegetation was high 0.1921 and shrub land 0.155. The least NDVI mean value was recorded for Dry River 0.1223 and barren land 0.1287.

Analysis of Land Surface Temperature

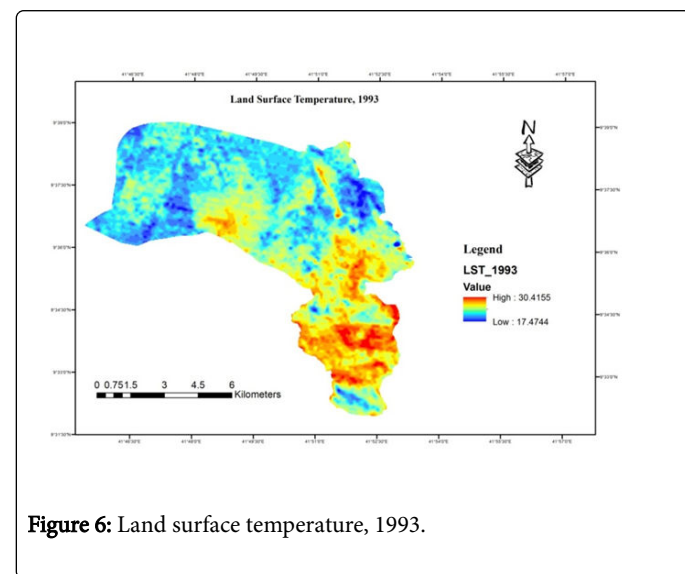


Figure 6: Land surface temperature, 1993.

Class No.	Class Name	Count	Area/km ²	LST, 1993				LST, 2017			
				Min	Max	Mean	STD	Min	Max	Mean	STD
1	Built Up	14183	3.19	17.93	30.42	26.61	1.31	23.43	33.23	26.53	1.91

2	Sparse Vegetation	12328	2.77	17.47	30	26.03	1.48	22.57	33.69	26.03	2.07
3	Shrub Land	18157	4.09	23.25	29.59	25.43	1.02	23.75	27.72	24.57	0.60
4	Barren Land	48705	10.96	20.17	30.42	26.23	1.35	22.95	32.92	26.59	1.44
5	Dry River	1159	0.26	22.81	30	25.93	1.81	22.93	33.31	26.29	1.98

Table 9: Land Surface Temperature (LST) 1993-2017.

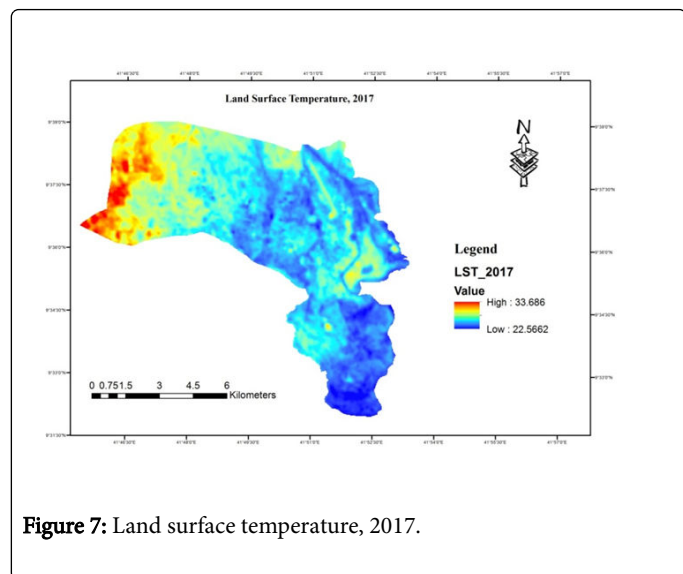


Figure 7: Land surface temperature, 2017.

Land surface temperature was derived from Landsat imagery (TM and OLI/TIRS). LST was estimated using conversion of radiance to At satellite brightness temperature and spectral emissivity.

Table 9 shows, in 1993 maximum temperature was recorded 30.42°C with minimum temperature value of 17.47°C. On the other hand, on 2017, the highest temperature recorded was 33.69°C and the lowest temperature was 22.57°C. Therefore, the average LST of overall area for the two observation years has increase from 23.95°C to 28.12°C.

Table 9 shows the estimated value of five major LULC categories. Accordingly, in 1993 built up area exhibit the highest LST having mean value of 26.61°C with a standard deviation of 1.31. Barren land has also exhibited highest LST with a mean value of 26.23°C and standard deviation of 1.35. On the other side, shrub land and Dry River show lower LST having a mean value of 25.43°C and 25.93°C with a standard deviation of 1.02 and 1.81 respectively. In 2017, the estimated (Figures 6 and 7).

LST value of barren land exceeds other LULC class with a mean value of 26.59°C and standard deviation of 1.44. Built up area has also exhibit the second highest LST value having mean of 26.5°C and standard deviation of 1.9. On the other hand, shrub land shows the lowest LST value having mean of 24.57°C and standard deviation of 0.60. Other scholar has also witnessed it also shows that the highest values of LST are in the urban or built-up area and other impervious surfaces while the lower LST values are found around vegetated areas [23]. Vegetative covers absorb heat during the daytime and release it at night as a result low value of LST is commonly recorded in such LULC type [24]. The temperature value around residential site, industrial

shades and parks, road networks, and concrete pavements become considerably higher than barren land. Nevertheless, urban built up areas geographically proximate to shrub land sparse vegetation shows relatively low LST value because of coarser spatial resolution of satellite imagery used.

Correlation of LST and NDVI

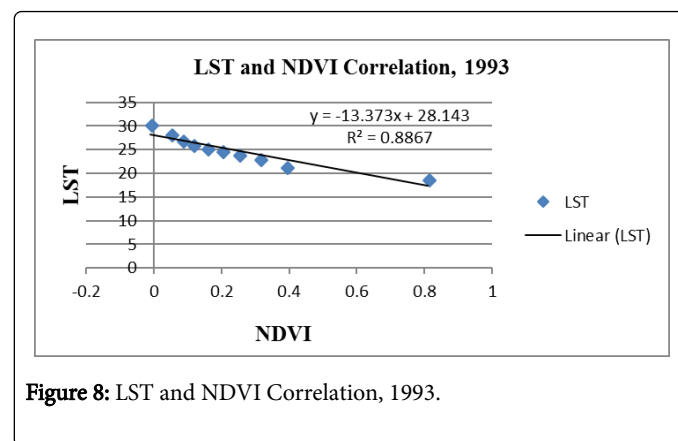


Figure 8: LST and NDVI Correlation, 1993.

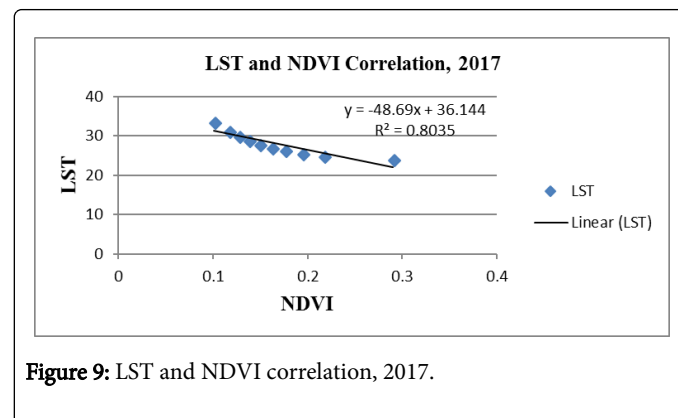


Figure 9: LST and NDVI correlation, 2017.

Tables 8 and 9, above shows the relationship of NDVI and LST. It can reveal that, those LULC classes that have higher LST values have shown lowest NDVI value. This is due to surface radiant temperature value is negatively correlated with NDVI value for all land use type. As a result, the highest NDVI value and lowest LST is observed in land cover with high vegetation and vice versa [25]. Therefore, shrub land (25.43°C in 1993 and 24.57 in 2017) and sparse vegetation (26.03°C in 1993 and 26.03°C in 2017) depict lowest mean LST value and high NDVI mean value for both study years. From Figures above Figures 8 and 9 also shows that, LST and NDVI for both study years have strong negative correlation with R square value of 0.886 and 0.803 respectively.

LULC Change and Relationship with LST

Form Table 9 non-evaporating surfaces that comprises built up area and barren land has relatively high surface radiance temperature. With a rapid rate of urban growth and expansion of settlement, surface radiance temperature of built up area become the leading from LULC classes. It is also indicate that, non evaporating surface such as metals, concrete, sand stone release more heat than green plants having high NDVI value [9]. Even though, the LULC change of shrub land disclose rapid expansion rate, the amount of surface radiant temperature is still low and minimum as compared to built up areas.

The average value of LST for Built up area has exhibited difference from 24.175°C in 1993 to 28.33°C in 2017. Areal extent of shrub land was in increasing trend and since shrub land has higher NDVI value, the LST mean value has decreased from 25.43°C in 1993 to 24.57°C in 2017. Therefore, with the expansion of vegetated area the LST value adversely decrease and the expansion of non- evaporating surface brought increase in LST. Increase in density of settlement, reduction in open space and green cover, increase in built up space improves the LST of urban area [2]. With the rapid growth and expansion of urban area, the propensity for conversion of LULC in to built up area and dwelling unit (non-evaporating surface) becomes high. Thus, such surfaces have high probability for showing greater value of LST.

Conclusion

In this study the spatial distribution of land surface temperature in terms of land use land cover change and NDVI was analyze. The study use TM, 1993 and OLI/TIRS, 2017 landsat images and images has classified in to five major LULC categories. The result shows that, for the last 25 years, the portion of land under built up area and shrub land have shown significant expansion due to urban growth and alien green pant expansion particularly *Prosopis juliflora*. On the other hand, barren land has shown considerably high rate of conversion and decrease in territorial extent from 1993 to 2017. With regard to LST, result implies it has strong negative correlation with NDVI. More vegetated area like sparse vegetation and shrub land classes have shown lowest LST value and high NDVI and vice versa. According to the result of the study, highest mean value of LST was recorded in built up LULC class since built up area is covered with surface of concrete, iron sheet, house, road, and pavements. Barren land also exhibited highest LST value due to high accumulation of sandy soil. Therefore, with the conversion of land from vegetated area to built up area, LST depicts highest value.

Acknowledgment

The author would like to thank Mr. Nigus and Mr. Tesfaye for their help in various ways.

References

1. Mahmood R, Pielke Sr RA, Hubbard KG, Niyogi D, Bonan G, et al. (2010) Impacts of land use/land cover change on climate and future research priorities. Bulletin of the American Meteorological Society 91: 37-46.
2. Lilly Rose A, Devadas MD (2009) Analysis of land surface temperature and land use/land cover types using remote sensing imagery-a case in Chennai city, India. In The seventh International Conference on Urban Clim.
3. Coskun HG, Alganci U, Usta G (2008) Analysis of land use change and urbanization in the Kucukcekmece water basin (Istanbul, Turkey) with temporal satellite data using remote sensing and GIS. Sensors 8: 7213-7223.
4. Jiang J, Tian G (2010) Analysis of the impact of land use/land cover change on land surface temperature with remote sensing. Procedia Environmental Sciences 2: 571-575.
5. Igun E, Williams M (2018) Impact of urban land cover change on land surface temperature. Global Journal of Environmental Science and Management 4: 47-58.
6. Alshaikh A (2015) Vegetation cover density and land surface temperature interrelationship using satellite data, case study of Wadi Bisha, South KSA. Advances in Remote Sensing 4: 248-262.
7. Alqurashi AF, Kumar L (2013) Investigating the use of remote sensing and GIS techniques to detect land use and land cover change: A review. Advances in Remote Sensing 2: 193-204.
8. Sahana M, Ahmed R, Sajjad H (2016) Analyzing land surface temperature distribution in response to land use/land cover change using split window algorithm and spectral radiance model in Sundarban Biosphere Reserve, India. Modeling Earth Systems and Environment 2: 81.
9. Saleh SA (2010) Impact of urban expansion on surface temperature in Baghdad, Iraq using remote sensing and GIS techniques. Journal of Al-Nahrain University-Science 13: 48-59.
10. Mallick YKBB, Kerle CAN (2006) Satellite-based Analysis of the Role of Land Use! Land Cover and Vegetation Density on Surface Temperature Regime of Delhi, India. J Indian Soc Remote Sens 37: 201-214.
11. Tali JA, Divya S, Murthy K (2013) Influence of urbanisation on the land use change: A case study of Srinagar City. Am J Res Commun 1: 271-283.
12. Hashim N, Ahmad A, Abdullah M (2007) Mapping urban heat island phenomenon, remote sensing approach. Journal-The Institution of Engineers, Malaysia 68: 25-30.
13. Dire Dawa Finance Economy Development Bureau (2016) Dire Dawa Administration Statistical Abstract 2013-2015. Dire Dawa, Ethiopia.
14. Dire Dawa Administrative Council Water Mines & Energy Office (2012) Dire Dawa Administrative Council Integrated Resource Development Master Plan Study Project. Addis Ababa, Ethiopia.
15. Tessema YA (2012) Ecological and economic dimensions of the paradoxical invasive species-Prosopis juliflora and policy challenges in Ethiopia. Journal of Economics and Sustainable Development 3: 62-71.
16. Zeray N, Legesse B, Mohamed JH, Aredo MK (2017) Impacts of Prosopis juliflora invasion on livelihoods of pastoral and agro-pastoral households of Dire Dawa Administration, Ethiopia. Pastoralism 7: 7.
17. FAO (2006) Problem Posed by the Introduction of Prosopis Spp in Selected Countries. Rome, Italy.
18. Pan S, Li G, Yang Q, Ouyang Z, Lockaby G, et al. (2013) Monitoring land-use and land-cover change in the Eastern Gulf Coastal Plain using multi-temporal Landsat imagery. J Geophys Remote Sens 2: 2169-2249.
19. Study for Swiss Agency for Development and Cooperation (2017) Urban and Peri- Urban Development Dynamics in Ethiopia Study for Swiss Agency for Development and Cooperation. Addis Ababa, Ethiopia.
20. Mohan M, Pathan SK, Narendrareddy K, Kandya A, Pandey S (2011) Dynamics of urbanization and its impact on land-use/land-cover: a case study of megacity Delhi. Journal of Environmental Protection 2: 1274-1283.
21. Nayak BK (2013) The Plight of Slum Dwellers at Gondar City in Ethiopia. International Journal of Management and Social Sciences Research 2: 56-63.
22. Gandhi GM, Parthiban S, Thummalu N, Christy A (2015) Ndvi: Vegetation change detection using remote sensing and GIS-A case study of Vellore district. Procedia Computer Science 57: 1199-1210.
23. Nzoiwu CP, Agulue EI, Mbah S, Igboanugo CP (2017) Impact of Land Use/Land Cover Change on Surface Temperature Condition of Awka Town, Nigeria. Journal of Geographic Information System 9: 763-776.
24. Surawar M, Kotharkar R (2017) Assessment of Urban Heat Island through Remote Sensing in Nagpur Urban Area Using Landsat 7 ETM+ Satellite Images. World Academy of Science, Engineering and

- Technology, *International Journal of Civil, Environmental, Structural, Construction and Architectural Engineering* 11: 868-874.
25. Omran ESE (2012) Detection of land-use and surface temperature change at different resolutions. *Journal of Geographic Information System* 4: 189-203.